


Cite this: *RSC Adv.*, 2021, 11, 18818

# Facile synthesis of novel dopamine-modified glass fibers for improving alkali resistance of fibers and flexural strength of fiber-reinforced cement

Pengfei Ma,<sup>a</sup> Minglian Xin,<sup>b</sup> Yan Zhang,<sup>c</sup> Shenguang Ge,<sup>d</sup> Dan Wang,<sup>a</sup> Congcong Jiang,<sup>a</sup> Lina Zhang<sup>\*a</sup> and Xin Cheng<sup>\*a</sup>

Glass fiber-reinforced cementitious material is one of the significant components in structural materials playing vital roles in enhancing the tensile and flexural behavior of cement-based quasi-brittle materials. Compared with carbon and polymer fibers, its intrinsic similar silicate-based composition to cement was endowed with better bonding properties and compatibility with cement-based materials. However, the poor alkali resistance of glass fibers restrained their potential development for spreading to applications in construction fields. In this study, dopamine-modified glass fibers (DP) were self-polymerized at ambient temperature by a facile method for enhancing the alkali resistance of glass fibers. Scanning electron microscopy and X-ray photoelectron spectroscopy were utilized for characterizing DP. The duration of reaction and fiber to solution ratio were adjusted with an optimal reaction time of 12 h and fiber to solution ratio of 0.12 g ml<sup>-1</sup> acquired. Alkali resistance was measured by strength retention tests in both mortar and sodium hydroxide solution. Compared with untreated glass fibers (UN), DP exhibited a distinct improvement in strength retention rate of 37.1% and 18.9% under mortar and sodium hydroxide solution environments, respectively. Also, flexural strength tests of DP-reinforced cement were conducted, and its strength was increased in comparison with that of UN-reinforced cement by 58.2%. As a consequence, a novel simple method for improving the alkali resistance of glass fibers was proposed and is anticipated to promote the development and applications of glass-fiber reinforced cement-based materials.

Received 10th March 2021

Accepted 3rd May 2021

DOI: 10.1039/d1ra01875b

rsc.li/rsc-advances

## 1. Introduction

Cement and concrete materials have been prevalently used in universal construction applications due to their cost-effectiveness, widespread availability, unparalleled strength, durability, longevity and resilience and so forth.<sup>1,2</sup> Nevertheless, their poor tensile strength and toughness, low specific strength and ease of crack formation restrained their advanced development to a great extent.<sup>3</sup> Incorporation of fibers is one of the most significant and effective ways to compensate for such limitations, and could help in enhancing their mechanical properties and durability.<sup>4</sup> Diverse types of fibers have been successfully utilized in cement and concrete in terms of their

chemical composition such as carbon fibers, PVA fibers, steel fibers, basalt fibers, *etc.*<sup>5–11</sup>

Glass fibers with the merits of high tensile strength and elastic modulus, good flexibility, superior weather resistance, good compatibility and non-combustibility, have been gradually applied in cement and concrete.<sup>5,12–15</sup> Taking the role of 'bridging counterpart and inhibitor', they can distinctly both strengthen tensile and flexural behavior and reduce cracking and shrinkage of cement and concrete.<sup>16</sup> Zhou *et al.*<sup>17</sup> explored the effect of glass fibers on the workability and mechanical properties of mortar. Results showed that flexural strength of mortar at 28 days increased by nearly 80.4%. Tassew and Lubell<sup>18</sup> founded that though having moderating influence on the compressive strength and elastic modulus on ceramsite concrete, chopped glass fibers took strong effect on boosting its shear strength by nearly 40%. Barluenga *et al.*<sup>19</sup> discovered that chopped glass fibers were sufficient for restraining shrinkage. The introduction of chopped glass fibers could reduce crack area and maximum crack length of concrete. Compared with reference concrete, the glass fiber-reinforced concrete exhibited distinct reduction of 6.9–94.5% and 85.4–97.2% in crack area and the maximum crack length, respectively.

<sup>a</sup>Shandong Provincial Key Laboratory of Preparation and Measurement of Building Materials, University of Jinan, Jinan 250022, Shandong, China. E-mail: mse\_zhangln@ujn.edu.cn

<sup>b</sup>Shandong Hi-speed Road & Bridge International Engineering Co. Ltd., Jinan 250014, Shandong, China

<sup>c</sup>School of Chemistry and Chemical Engineering, University of Jinan, Jinan 250022, Shandong, China

<sup>d</sup>Institute for Advanced Interdisciplinary Research, University of Jinan, Jinan 250022, Shandong, China



However, drawbacks on poor alkaline resistance of glass fibers and weak interfacial bonding between fibers and cement are still of great necessity to be solved. Especially, the deterioration of glass fibers under alkaline environment severely hinders their long-term service in cement and concrete materials. Many studies have confirmed that basic solution was aggressive to glass fibers.<sup>20–22</sup> Under high pH ( $\geq 10.5$ ) surrounding, the silicate-network of glass fibers was sensitively broken by hydroxyl ions present in high quantity and thus the strength was degraded accordingly. With the increment of the concentration of hydroxyl ions, the destruction rate of silicate-network of glass fibers was accelerated steeply and the erosion effect performs more severe. When serving in cement and concrete possessing typical pH value greater than 12.5, the decay of glass fibers was the most concerning issue which results in the strength and durability of glass fibers far beneath their theoretical values.<sup>23–25</sup> As a consequence, various measures have been taken to remedy such adverse performance. The development of alkali-resistant glass fibers was considered to be effective approach which was based on the adjustment of chemical composition.<sup>26–29</sup> It is delighting that such took effect on acquisition of enhancement of alkali resistance for glass fibers, still satisfaction cannot be in pace with that of cement and concrete materials with respect to long-term service. Surface modification was another significant strategy which could also be beneficial to the strengthening of interfacial bridging between fibers and cement matrix that was equally crucial factor to fibers. Hence, a variety of surface modification schemes have as well been proposed for adjustment of both alkaline resistance and interfacial bonding between fibers and cement, including etching, coating, surface grafting, plasma treatment and so forth.<sup>30–35</sup> Mader *et al.*<sup>36</sup> founded that corrosion process of hydroxyl ions on glass fibers could be delayed after coating with organic polymer. Under the action of hydroxyl ions, the thickness of sizing agent layer on the surface of glass fibers decreased sharply. Fortunately, this process ceased after a period of time and the remaining thickness of sizing agent layer accounted for about 30% of the initial thickness, which continued to be capable of providing protection for fibers. Gao *et al.*<sup>37</sup> coated the surface of glass fibers with silane coupling agent. Results showed that tensile strength of coated glass fibers was 30% higher than that of the untreated ones after being immersed in the same concentration of alkali solution for a period of time. Nevertheless, most of the approach currently suffered from complex process, high cost, weak bonding, ease of additional damage to fibers.

Nanomaterials possesses distinguished features of large surface-area-to-volume ratio, high chemical reactivity, diversely adjustable and controllable structure and morphology that have been successfully applied in many fields.<sup>38</sup> As operative and controllable modification candidates, nanomaterials are capable of acting as protective layer as well as whisker-like branched structure on the surface of fibers, resulting in better resistance of fibers to hazardous surroundings and improvement of interfacial bonding between fibers and cement-based materials. Correspondingly, the mechanical properties and interfacial structure of fiber-reinforced cement composites were

effectively enhanced.<sup>39</sup> Liu *et al.*<sup>40</sup> treated glass fibers with nano-clay *via* surface coating. They soaked those modified glass fibers and untreated ones in different alkaline solutions (NaOH, KOH,  $\text{Ca}(\text{OH})_2$ ) with pH value of 13.5 (simulating the hydration environment of concrete) for varied duration, and observed the surface morphology of glass fibers by scanning electron microscope (SEM). Results showed that nano-clay formed a protective layer on the surface of glass fibers, which could credibly delay the corrosion attacked from hydroxyl ions and improve their alkali resistance. Gao *et al.*<sup>41</sup> also founded that nano-clay improved the alkali corrosion resistance of glass fibers *via* surface coating. Wei *et al.*<sup>42</sup> modified basalt fibers with coating of nano-silica for enhancement of epoxy matrix. It was showed that not only tensile strength of modified basalt fibers increased by 30%, but the interfacial shear strength of basalt fiber/resin composites raised by 15%. Such could be due to the introduction of nano-silica particles which strengthened the roughness of fibers as well as the interfacial adhesion between fibers and matrix. Rahaman *et al.*<sup>43</sup> utilized carbon nanotubes to modify glass fiber/epoxy resin. The results indicated that modification of carbon nanomaterials improved the adhesion between glass fibers and polymer matrix and contributed to the elevation of storage modulus of fibers by 38%. Faranak *et al.*<sup>44</sup> conducted modification of bagasse fibers *via* the introduction of bacteria which resulted in deposition of nanocellulose on the surface of bagasse fibers and improved interfacial adhesion between bagasse fiber and cement matrix correspondingly. In our previous work, trials on modification of dopamine was also rudimentary studied with its effect on shrinkage properties of cement included. Such preliminary results explored our views on utilization of nanomodification in fiber-reinforced cement.<sup>45</sup>

Founded on availability of nanomodification of fibers and our previous work, in this paper, dopamine was *in situ* self-polymerized on the surface of fibers at ambient temperature by a facile solution reaction and characterized SEM and X-ray photoelectron spectroscopy (XPS). The duration of reaction and fiber to solution ratio were adjusted to acquire optimal preparation conditions. Alkali resistance of as-prepared glass fibers were further investigated *via* strength retention (SIC) test in mortar and strength retention ratio test in sodium hydroxide solution. Subsequently, as-prepared dopamine-modified glass fibers (DP) were incorporated under varied quantities into cement slurry with different w/c ratio for studying their effect on flexural strength of cement.

## 2. Methodology

### 2.1 Materials

Dopamine hydrochloride, tris(hydroxymethyl)aminomethane (Tris) and sodium hydroxide in analytical grade were bought from Sigma-Aldrich, USA. Hydrochloric acid in 12 M was purchased from Laiyang Economic and Technological Development Zone Fine Chemicals, China. Chopped glass fibers (Cem-FIL60, length: 12 mm, density:  $2.68 \text{ g cm}^{-3}$ ), glass fiber strands (AR5325, tex: 1200, density:  $2.60 \text{ g cm}^{-3}$ ) and woven fabrics (EFF7630, weight:  $230 \text{ g m}^{-2}$ ) were purchased from Taishan Glass Fiber Co. Ltd, China. Ordinary Portland cement



42.5 (equivalent to European CEM I 42.5) was acquired from Shandong Sunnsy Cement Group Co. Ltd, China. Distilled water was purified from water purification system (Millipore Direct-Q 8, Germany) that was utilized for the preparation of DP.

## 2.2 Sample preparation

0.3 M Tris and 0.2 M hydrochloric acid solution were mixed together to attain Tris-HCl buffer solution with pH value set at 8.5. With the concentration of dopamine hydrochloride controlled at  $2 \times 10^{-3} \text{ g ml}^{-1}$  in Tris-HCl buffer solution, certain quantities of glass fibers were added into Tris-HCl buffer solution at varied fiber to solution ratio. The reaction undergone in water bath thermostat at  $20^\circ\text{C}$  for different timeslot with adequate oxygen provided. Subsequently, glass fibers were washed by distilled water until pH value of the solution washed became neutral, dried at  $60^\circ\text{C}$  for 48 h, and stored for further use. Detailed DP information was listed in Table 1.

The preparation of samples for SIC test followed EN14649: 2005(E). A glass fiber strand in length of 20 cm was laid across the central portion of the mold in dimensions of  $30 \times 10 \times 10 \text{ mm}$  and held under slight tension by means of adhesive tape. Epoxy resin was subsequently applied as a coating on to the strand, leaving the central test length of 30 cm uncoated. After the resin was cured, a small quantity of silicone sealant was placed around the strand as grommet at the point where the resin impregnated portion ended and the test length began for blocking the mortar impregnation. Mortar in mix proportion of cement : water : sand (c : w : s) equaling to 1 : 0.43 : 0.33 was then mixed thoroughly and placed inside the mold and tapped for ensuring complete filling. The mold was subsequently placed in standard curing ( $20^\circ\text{C}/\text{RH } 95\%$ ) for 24 h before demolding. The demolded samples were finally immersed in distilled water at  $80^\circ\text{C}$  for 96 h and then at  $20^\circ\text{C}$  for 15 min. Herein, high temperature was utilized as accelerated aging process for evaluating long-term alkali resistance of fibers, while cooling down process was to cease accelerated aging for subsequent measurement of SIC strength.

The samples of woven fabrics for strength retention ratio study were made based on GB/T 20102-2006. Woven fabrics in dimensions of  $600 \times 50 \text{ mm}$  were cut into two pieces; each in

dimension of  $300 \times 50 \text{ mm}$  possessed same numbers of warp and weft. One piece was immersed into 5 wt% sodium hydroxide solution at  $23^\circ\text{C}$  for 28 d, then washed with distilled water and finally put in ambient environment ( $23^\circ\text{C}/\text{RH } 50\%$ ) for another 7 d. The another piece was placed in ambient environment ( $23^\circ\text{C}/\text{RH } 50\%$ ) for 35 d as comparison.

Fiber-reinforced cement samples were mixed in w/c of 0.3, 0.35 and 0.4 with fiber volume set at 0%, 1%, 3%, 5% and 7%, respectively and were cast in molds of  $160 \times 40 \times 40 \text{ mm}$ . All samples were cured for 28 d in standard curing chamber ( $20^\circ\text{C}/\text{RH } 98\%$ ).

## 2.3 Testing methods

Morphology of DP was obtained *via* SEM (FEI, QUANTA FEG 250). Surface composition of the glass fibers was characterized by XPS (Thermo Fisher SCIENTIFIC, ESCALAB 250) with full scan and high-resolution scan spectra measured. The analysis of C 1s, N 1s, and O 1s was exerted using XPSPEAK41 software with Gaussian-Lorentzian function. After subtraction of a Shirley background, the peak-fitting procedure was conducted. Best fit with minimum number of peaks was acquired based on comprehensive consideration of peak position, full width at half-maximum (FWHM), as well as intensity. SIC strength of glass fiber strand and strength retention ratio of woven fabrics were tested by a universal testing machine (MTS Systems, E42) with maximum capacity of 5 kN at a loading speed of  $1 \text{ mm min}^{-1}$  and  $100 \text{ mm min}^{-1}$ , respectively. The SIC strength was calculated by eqn (1),

$$\sigma = \frac{F}{M} \times \rho \quad (1)$$

in which  $F$  represented failure load,  $M$  was weight of the adjacent 1 m length of strand, and  $\rho$  stood for density of glass fibers. Each measurement was the average value from eleven repeated experiments. Strength retention ratio was calculated by eqn (2) and gained averagely from eight samples for each measurement,

$$R = \frac{\sum \frac{F_n}{U_n}}{n} \times 100\% \quad (2)$$

where  $F$  was the load measured for the piece of woven fabrics immersed in sodium hydroxide solution,  $U$  was the other piece without alkaline erosion, and  $n$  represented the number of samples. Flexural strength was conducted using a universal testing machine (MTS Systems, CMT5504) with maximum capacity of 50 kN at a loading speed of  $0.3 \text{ kN s}^{-1}$ . The average value was acquired from six parallel samples for each mix proportion.

## 3. Results and discussion

### 3.1 Modification of glass fibers with dopamine

Fig. 1 illustrated SEM images of DP under varied duration of polymerization. The appearance of DP was light brown (Fig. 1f) which was easily distinguishable from that of UN in faint color. Compared with UN (Fig. 1a), nanoparticles were obviously

Table 1 DP information

| Sample denotation    | Fiber to solution ratio ( $\text{g ml}^{-1}$ ) | Duration of reaction (h) |
|----------------------|--|--------------------------|
| UN (untreated)       | 0  | 0                        |
| DP12-04 <sup>a</sup> | 0.12   | 4                        |
| DP12-08 <sup>a</sup> | 0.12   | 8                        |
| DP12-12 <sup>a</sup> | 0.12   | 12                       |
| DP12-24 <sup>a</sup> | 0.12   | 24                       |
| DP16-12 <sup>a</sup> | 0.16   | 12                       |
| DP08-12 <sup>a</sup> | 0.08   | 12                       |
| DP04-12 <sup>a</sup> | 0.04   | 12                       |

<sup>a</sup> DPX-Y: X, fiber to solution ratio; Y, reaction time.



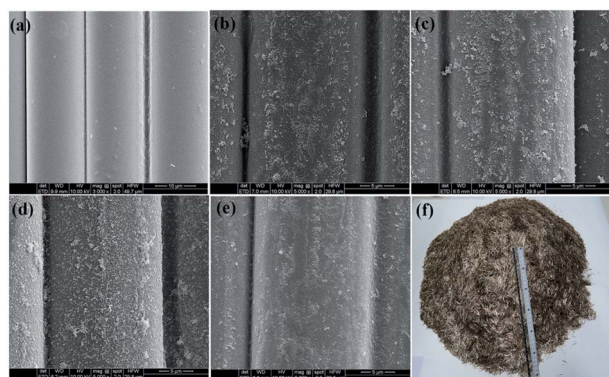


Fig. 1 SEM images of (a) UN; (b) DP12-04; (c) DP12-08; (d) DP12-12; (e) DP12-24 and (f) photograph of as-developed DP. (DPX-Y: X, fiber to solution ratio; Y, reaction time.)

visible when dopamine polymerization was conducted, indicating the formation of new product on the surface of glass fibers. The XPS survey spectra and high-resolution scan spectra over C 1s, N 1s and O 1s of UN and DP were illustrated in Fig. 2. As was noted in Fig. 2a, UN contained the elements of silicon, oxygen, sodium, zirconium and carbon. The C 1s spectrum displayed in Fig. 2b was fitted with C-C which was attributed to adventitious carbon at 284.8 eV.<sup>46</sup> The O 1s spectrum in Fig. 2c represented one peak located at 532.7 eV which was assigned to O-Si-O from glass fibers.<sup>47</sup> Comparatively in DP shown in Fig. 2a, element of zirconium disappeared while that of

nitrogen emerged after modification process was exerted, suggesting the formation of *in situ* polymerized dopamine. In terms of C 1s spectrum (Fig. 2d), three characteristic peaks were clearly distinguished which were related to C-C, C-O/C-N and C=O bond at 284.8 eV, 285.6 eV and 287.7 eV, respectively. Among them C-C was the same as that shown in UN which was mostly owing to adventitious carbon. Additional C-O/C-N and C=O bond came from emerging polydopamine, which could be contributed from secondary and tertiary amine species in cyclization and polymerization of dopamine while C=O bond could be contributed to oxidation of dopamine, which were coincided with those reported.<sup>48,49</sup> Two characteristic peaks were attained in N 1s spectrum (Fig. 2e) which could be originated from R-NH<sub>2</sub> (399.5 eV) and C-N (400.2 eV) in amine species and cyclization of polydopamine.<sup>50-52</sup> Also in O 1s spectrum two characteristic peaks were displayed (Fig. 2f) which accounted for C=O (531.0 eV) and O-Si-O/C-O (532.7 eV).<sup>47</sup> The former was found in oxidation of dopamine while the latter was from glass fibers and polydopamine. Detailed assignment was summarized in Table 2. As a consequence, founded on oxidation, cyclization and polymerization of dopamine,<sup>52</sup> successful acquisition of self-polymerized DP could be clearly manifested.

Additionally, such modification became gradually thorough accompanied with the prolonging of reaction as was seen in Fig. 1. After reacting for 4 h (Fig. 1b), polydopamine in nano-scale were locally formed in uneven distribution. With polymerization process extended to 8 h (Fig. 1c), almost a layer of covering could be obviously observed on the surface of glass fibers. Prolonging the polymerization for another 4 h (Fig. 1d), the surface of fibers was fully covered with a layer of relatively uniform and dense nanomaterials. Nevertheless, with further extension of reaction, film-like product was gained which reversely reduced surface roughness to some extent (Fig. 1e). As a consequence, 12 h was currently selected to be optimal duration of dopamine polymerization.

Fig. 3 showed SEM images of DP under varied fiber to solution ratio with polymerization of dopamine all occurring for 12 h. At larger fiber to solution ratio (Fig. 3a), limited quantities of nanomaterials were found and the surface of glass fibers could not be completely enclosed. Decreasing the fiber to solution ratio (Fig. 3b) gradually resulted in more distinctive formation of product layer. However, when the fiber quantity was further lowered down (Fig. 3c and d), smaller particles were additionally observed and easily agglomerated reducing the evenness of the particles on the surface of fibers distinctly. As a result, fiber to solution ratio was optimally set at 0.12 g ml<sup>-1</sup>.

### 3.2 Alkaline resistance of dopamine-modified glass fibers

Fig. 4 showed the SIC strength for glass fiber strands. Among all the samples prepared, UN exhibited lowest SIC strength, suggesting the effective enhancement on alkali resistance of DP. The decrement of fiber to solution ratio and extended duration of reaction both resulted in larger SIC strength, which was in accordance with SEM images gained in 3.1 that more polydopamine encompassed the surface of glass fibers which reacted as protective layer. The SIC strength of DP12-04, DP12-08, DP12-12

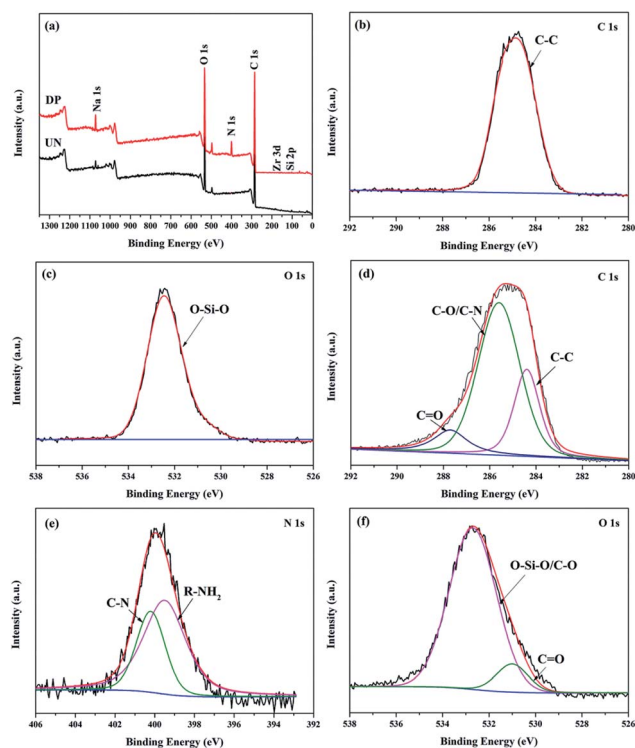


Fig. 2 (a) XPS survey spectra and high-resolution scan spectra of (b) C 1s in UN; (c) O 1s in UN; (d) C 1s in DP; (e) N 1s in DP and (f) O 1s in DP.





Table 2 Detailed information of XPS results

| Sample | Element | Group             | BE <sup>a</sup> (eV) | FWHM (eV) | Area (P) CPS.eV | Ref.      |
|--------|---------|-------------------|----------------------|-----------|-----------------|-----------|
| UN     | C 1s    | C-C               | 284.8                | 1.875     | 30 531.710      | 46        |
|        | O 1s    | O-Si-O            | 532.7                | 1.600     | 40 251.900      | 47        |
| DP     | C 1s    | C-C               | 284.8                | 1.300     | 12 590.720      | 48 and 49 |
|        |         | C-O/C-N           | 285.6                | 2.120     | 32 423.630      |           |
|        |         | C=O               | 287.7                | 1.730     | 5273.321        |           |
|        | N 1s    | R-NH <sub>2</sub> | 399.5                | 2.500     | 4524.323        | 50–52     |
|        |         | C-N               | 400.2                | 1.700     | 2348.640        |           |
|        |         | C=O               | 531.0                | 1.600     | 4165.241        | 47        |
|        | O 1s    | C=O               | 531.0                | 1.600     | 4165.241        |           |
|        |         | O-Si-O/C-O        | 532.7                | 2.400     | 34 449.830      |           |

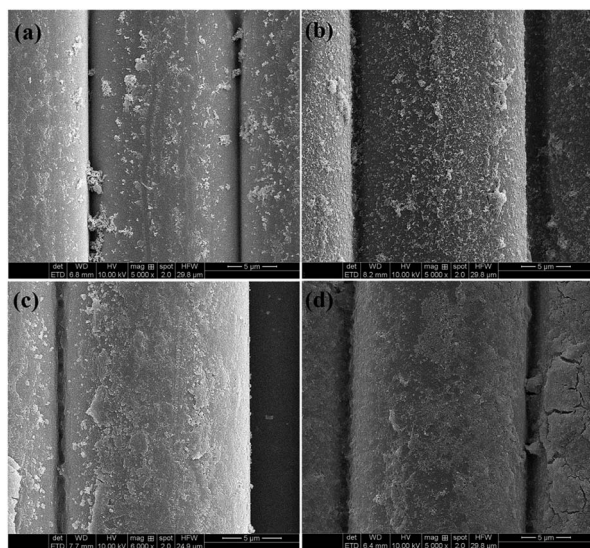
<sup>a</sup> BE: binding energy.

Fig. 3 SEM images of (a) DP16-12, (b) DP12-12, (c) DP08-12 and (d) DP04-12. (DPX-Y: X, fiber to solution ratio; Y, reaction time.)

and DP12-24 shown in Fig. 4a increased by 11.2%, 24.6%, 36.9% and 37.1%, respectively compared with that of UN. DP12-04 exhibited minimum enhancement which could be due to inadequate formation of self-polymerized dopamine within short reacting period and thus insufficient protecting effect. Accompanied with the extending of reaction, more polydopamine were produced and accordingly SIC strength arose distinctively. Such obvious increasing extent could also indicate

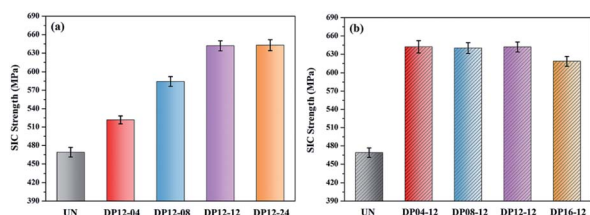


Fig. 4 SIC strength of glass fiber strands under variation of (a) reaction time and (b) fiber to solution ratio. (DPX-Y: X, fiber to solution ratio; Y, reaction time. Error bars: coefficient of variance for eleven parallel samples.)

the sensitive influence of duration of reaction on the strengthening of alkali resistance of glass fibers. Compared with DP12-12, DP12-24 showed slight increment, which could be reflected from SEM images that the surface of DP12-12 had been substantially formed with polydopamine that took effect and additional production of polydopamine on DP12-24 could merely help enhance the alkaline resistance in minor extent whilst the duration of reaction doubled. With respect to fiber to solution ratio seen in Fig. 4b, DP16-12 performed remarkable enhancement by 31.9% by comparing with UN. Although a further increment by 5.0% was acquired for DP12-12, decreasing the fiber to solution ratio on the whole resulted in similar SIC strength with limited variation among DP12-12, DP08-12 and DP04-12, amplifying the adequate quantities of dopamine solution for polymerization on fibers when fiber to solution ratio was less than  $0.12 \text{ g ml}^{-1}$ . In comparison with SIC strength of DP12-04, DP12-08, DP12-12 and DP12-24, it could also be manifested that the effect of fiber to solution ratio did not exhibit as much influence as that of reaction time within the synthesized condition investigated herein and the highest improvement by 37.1% on SIC strength was acquired.

Fig. 5 illustrated the strength retention ratio of glass woven fabrics. All dopamine-modified samples possessed better strength retention ratio than that of UN with 62.2% attained. When fiber to solution ratio fell down as well as the reaction was prolonged, the strength retention ratio performed rising up to peak value of 81.1%, followed by slightly declining. Similar with results gained for SIC strength, in terms of duration of reaction

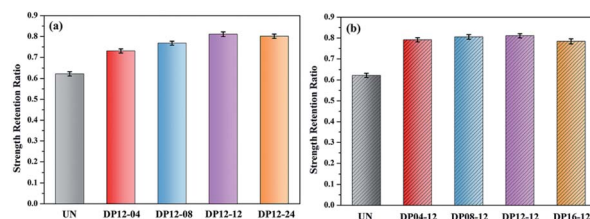


Fig. 5 The effect of (a) reaction time and (b) fiber to solution ratio on strength retention ratio of glass woven fabrics. (DPX-Y: X, fiber to solution ratio; Y, reaction time. Error bars: standard deviation for eight parallel samples.)



the strength retention ratio was elevated in appreciable extent by from 10.8% for DP12-04 to 18.9% for DP12-12, illuminating the positive effect on resistance to alkalis of fibers with polydopamine, saying that the addition of dopamine modification defended the body of glass fibers. A minor descending trend was illustrated for DP12-24 that improved by 17.9%. Analogously, a steep ascending was obtained for DP16-12 by 16.2%. However, after reaching up to supreme for DP12-12, a gradual drop of strength retention ratio was achieved accompanied by the reduction of fiber to solution ratio for DP08-12 and DP04-12. Such might be attributed to the agglomeration of dopamine polymerized or the unevenness of polydopamine based on SEM results obtained in 3.1 which were likely to bring adverse effect to small extent.

### 3.3 Effect of dopamine-modified glass fibers on flexural strength of cement

Fig. 6 presented flexural performance of fiber-reinforced cement. As was obviously observed, UN exhibited the lowest flexural strength under same w/c ratio and fiber content in general, suggesting the beneficial effect of self-polymerized dopamine on flexural behavior of glass fiber-reinforced cement which formed 'root whisker' structure on the surface of glass fibers.<sup>39</sup> The declining w/c ratio and ascending fiber content both conducted to enhanced flexural strength typically with the highest flexural strength obtained to be 15.35 MPa for sample prepared under w/c ratio of 0.3 and fiber content of 7%. Such tendency was in accordance with those reported

previously.<sup>53–57</sup> For one thing, the addition of glass fibers enhanced the 'bridge effect' on inhibition of microcrack propagation inside cement. For another, higher w/c ratio resulted in higher porosity on the whole and thus depreciation of flexural strength. For specified fiber content added or w/c ratio set, the flexural strength of cement was strengthened in varied extent predominantly. The steepest increment appeared within relatively smaller range of fiber content *i.e.* less than 3% for larger w/c ratio basically but at larger range for smaller w/c ratio. For instance, the strength of DP12-12 was approximately 1.85, 1.36 and 1.33 times of that of UN at w/c of 0.4, 0.35 and 0.3, respectively when 3% of fibers introduced but 1.35, 1.49 and 1.58 times of that of UN with 7% of fibers added accordingly. Such might be resulted from the compromise between effect of dopamine modification and content of fibers incorporated. As was widely reported more water promoted better dispersion of fibers and excessive incorporation of fibers adversely slowed down the strengthening effect to some extent<sup>53,58–60</sup> so that the optimal enhancement was attained in relatively smaller quantities of fiber incorporation, on which circumstance there might be slightly indistinct effect for modification of polydopamine. When w/c was lower, at higher fiber content more porosity was likely to be incorporated which facilitated the bridging effect between fiber reinforcements and cement matrix founded on modification of polydopamine and thus the enhancement effect of fibers to cement performed ascending. Additionally, the influence of fiber to solution ratio and extension of reaction time on flexural strengthening of cement were analogous primarily. The flexural strength of cement exhibited rising up to peak value followed by slightly declining when fiber to solution increased and the duration of reaction was prolonged basically, which was coincided with results aforementioned in Session 3.2. For instance, when w/c was set at 0.35 the flexural strength of DP16-12, DP12-12, DP08-12 and DP04-12 increased by 14.5%, 37.8%, 34.3% and 32.2% compared with that of UN, respectively and that of DP12-04, DP12-08, DP12-12 and DP12-24 was 13.2%, 30.1%, 37.8% and 35.7%, respectively. Shortened reaction time as well as larger fiber to solution ratio might consequently obtained insufficient formation of polydopamine on the surface of fibers and consequently limited enhancing effect. Abundant modification with adequate duration and reactants assisted cement slurry in strength improvement manifestly. However, excessiveness of modification might unfavorably reduce the flexural performance which probably possessed relatively smaller surface roughness and detrimental agglomeration as was shown in SEM results attained. The highest flexural strength was as a consequence acquired for DP12-12 with optimal modification conditions which was improved by 58.2% compared with that of UN.

## 4. Conclusion

Founded on facile self-polymerization at ambient temperature, novel *in situ* modification of polydopamine on glass fibers was successfully developed. Variation of duration of reaction and fiber to solution ratio both resulted in evolution in surface morphology and alkali resistance of fibers as well as flexural

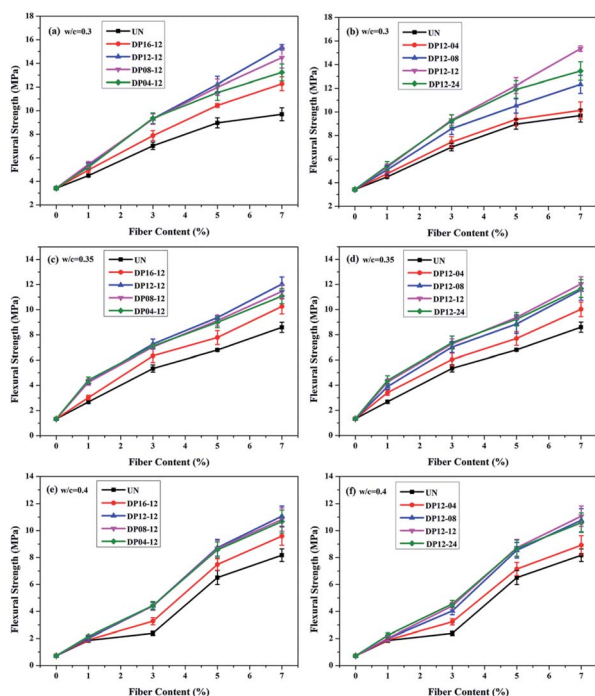


Fig. 6 Flexural performance of cement materials (fiber to solution ratio: (a), (c) and (e); reaction time: (b), (d) and (f)). (DPX-Y: X, fiber to solution; Y, reaction time. Error bars: standard deviation for six parallel samples.)



strength of cement. In substance, extended reaction time and lower fiber to solution ratio brought about massive addition of polydopamine formed which reacted as protective layer for hydroxyl attack in high alkaline environment and enhanced bridging mediator at the interface between fibers and cement arresting the expansion of micro-cracks inside the cement and improving flexural properties of cement. Additionally, under combinational effect of w/c ratio and fiber content, flexural strength of cement materials varied simultaneously. However, excessive growth could account for adverse effect on alkaline resistance of fibers and flexural strength of cement to some extent which might be due to the agglomeration of polydopamine produced that needed to be noticed. The optimal modification scheme was comprehensively built up at the duration of reaction to be 12 h and fiber to solution ratio 0.12 g ml<sup>-1</sup>, respectively with SIC strength and strength retention ratio of DP improved by 37.1% and 18.9% accordingly and flexural strength of DP-reinforced cement enhanced by 58.2% mostly in comparison with untreated ones. On the basis of aforementioned, it could be concluded the feasibility of nano-modification on surface of glass fibers was further explored. Also, as long as modification criteria was in appropriate adjustment and control, glass fibers *via in situ* modification of self-polymerized dopamine could be promising candidate for advancing applications of glass fibers in cement and developing high-performance cement-based materials.

## Conflicts of interest

There is no conflict of interest to declare.

## Acknowledgements

The authors would like to acknowledge the financial support from the National Natural Science Foundation of China (51872121, 51632003 and 51902129), Taishan Scholars Program, Case-by-Case Project for Top Outstanding Talents of Jinan, the Youth Innovation Support Program of Shandong Colleges and Universities (2019KJA017) and the 111 Project of International Corporation on Advanced Cement-based Materials (No. D17001).

## References

- 1 R. Laila, B. James, A. Rouhollah, M. Jon and S. Taijiro, Cement and Concrete Nanoscience and Nanotechnology, *Materials*, 2010, **3**, 918–942, DOI: 10.3390/ma3020918.
- 2 S. Florence and S. Konstantin, Nanotechnology in concrete – a review, *Constr. Build. Mater.*, 2010, **24**, 2060–2071, DOI: 10.1016/j.conbuildmat.2010.03.014.
- 3 Z. Pan, L. He, L. Qiu, H. K. Asghar, G. Li, J. W. Zhu, C. Frank, D. Li, W. H. Duan and M. C. Wang, Mechanical properties and microstructure of a graphene oxide-cement composite, *Cem. Concr. Compos.*, 2015, **58**, 140–147, DOI: 10.1016/j.cemconcomp.2015.02.001.
- 4 A. Peyvandi, P. Soroushian, N. Abdol and A. M. Balachandra, Surface-modified graphite nanomaterials for improved reinforcement efficiency in cementitious paste, *Carbon*, 2013, **63**, 175–186, DOI: 10.1016/j.carbon.2013.06.069.
- 5 Z. Xiong, Y. Zeng, L. G. Li, A. K. H. Kwan and S. H. He, Experimental study on the effects of glass fibres and expansive agent on the bond behaviour of glass/basalt FRP bars in seawater sea-sand concrete, *Constr. Build. Mater.*, 2021, **274**, 122100, DOI: 10.1016/j.conbuildmat.2020.122100.
- 6 P. Saravanakumar, M. Sivakamidevi, K. Meena and S. P. Yamini, An experimental study on hybrid fiber reinforced concrete beams subjected to torsion, *Mater. Today: Proc.*, 2021, DOI: 10.1016/j.matpr.2020.12.1003.
- 7 P. Subathra, D. S. Vijayan, R. Abirami, M. Kharsati and D. K. Das, Experimental investigation on concrete with marble dust and steel fiber, *AIP Conf. Proc.*, 2020, **2271**, 30016, DOI: 10.1063/5.0024779.
- 8 C. A. Juarez, G. Fajardo, S. Monroy, A. Duran-Herrera, P. Valdez and C. Magniont, Comparative study between natural and PVA fibers to reduce plastic shrinkage cracking in cement-based composite, *Constr. Build. Mater.*, 2015, **91**, 164–170, DOI: 10.1016/j.conbuildmat.2015.05.028.
- 9 C. Parinya, P. Wichit, I. Pitcharat, K. Nuntaporn and C. Nutthita, Feasibility Study of Using Basalt Fibers as the Reinforcement Phase in Fiber-Cement Products, *Key Eng. Mater.*, 2018, **766**, 252–257, DOI: 10.4028/www.scientific.net/KEM.766.252.
- 10 N. N. Kencanawati and M. Shigeishi, Acoustic Emission Hit Generation Behavior of Basalt Fiber High Strength Mortar under Compression, *Appl. Mech. Mater.*, 2014, **493**, 6, DOI: 10.4028/www.scientific.net/AMM.493.678.
- 11 V. Mechtcherine, A. Michel, M. Liebscher, S. Kai and C. Großmann, Mineral-impregnated carbon fiber composites as novel reinforcement for concrete construction: material and automation perspectives, *Autom. Constr.*, 2019, **110**, 103002, DOI: 10.1016/j.autcon.2019.103002.
- 12 C. S. Chowdhury, R. Prosser, T. W. Sirk, R. M. Elder and J. W. Gillespie, Glass fiber-epoxy interactions in the presence of silane: a molecular dynamics study, *Appl. Surf. Sci.*, 2021, **542**, 148738, DOI: 10.1016/j.apsusc.2020.148738.
- 13 W. C. Wang, H. Y. Wang, K. H. Chang and S. Y. Wang, Effect of high temperature on the strength and thermal conductivity of glass fiber concrete, *Constr. Build. Mater.*, 2020, **245**, 118387, DOI: 10.1016/j.conbuildmat.2020.118387.
- 14 J. K. Ganta, M. V. S. Rao, S. S. Mousavi, V. S. Reddy and C. Bhojarajuac, Hybrid steel/glass fiber-reinforced self-consolidating concrete considering packing factor: mechanical and durability characteristics, *Structures*, 2020, **28**, 956–972, DOI: 10.1016/j.istruc.2020.09.042.
- 15 Z. Wang, X. L. Zhao, G. Xian, G. Wu, R. K. S. Ramane and S. A. Saadi, Effect of sustained load and seawater and sea sand concrete environment on durability of basalt- and glass-fiber reinforced polymer (B/GFRP) bars, *Corros. Sci.*, 2018, **138**, 200–218, DOI: 10.1016/j.corsci.2018.04.002.
- 16 I. M. G. Bertelsen, L. M. Ottosen and G. Fischer, Influence of fiber characteristics on plastic shrinkage cracking in cement-based materials: a review, *Constr. Build. Mater.*, 2019, **230**, 116769, DOI: 10.1016/j.conbuildmat.2019.116769.





- 17 B. Y. Zhou, M. Zhang, L. Wang and G. W. Ma, Experimental study on mechanical property and microstructure of cement mortar reinforced with elaborately recycled GFRP fiber, *Cem. Concr. Compos.*, 2021, **117**, 103908, DOI: 10.1016/j.cemconcomp.2020.103908.
- 18 S. T. Tassew and A. S. Lubell, Mechanical properties of glass fiber reinforced ceramic concrete, *Constr. Build. Mater.*, 2014, **51**, 215–224, DOI: 10.1016/j.conbuildmat.2013.10.046.
- 19 G. Barluenga and F. Hernández-Olivares, Cracking control of concretes modified with short AR-glass fibers at early age. Experimental results on standard concrete and SCC, *Cem. Concr. Res.*, 2007, **37**, 1624–1638, DOI: 10.1016/j.cemconres.2007.08.019.
- 20 D. Xing, L. Chen, Q. Ma, B. Hao and P. C. Ma, What happens to glass fiber under extreme chemical conditions?, *J. Non-Cryst. Solids*, 2020, **548**, 120331, DOI: 10.1016/j.jnoncrysol.2020.120331.
- 21 W. Ouarhim, H. Essabir, M. O. Bensalah, N. Zari, R. Bouhfid and A. Qaissa, Structural laminated hybrid composites based on raffia and glass fibers: effect of alkali treatment, mechanical and thermal properties, *Composites, Part B*, 2018, **154**, 128–137, DOI: 10.1016/j.compositesb.2018.08.004.
- 22 V. Marcos-Meson, A. Michel, A. Solgaard, G. Fischer, C. Edvardsen and T. L. Skovhus, Corrosion resistance of steel fiber reinforced concrete – a literature review, *Cem. Concr. Res.*, 2017, **103**, 1–20, DOI: 10.1016/j.cemconres.2017.05.016.
- 23 J. Liu, M. Jiang, Y. Wang, G. Wu and Z. Wu, Tensile behaviors of ECR-glass and high strength glass fibers after NaOH treatment, *Ceram. Int.*, 2013, **39**, 9173–9178, DOI: 10.1016/j.ceramint.2013.05.018.
- 24 C. Scheffler, S. L. Gao, R. Plonka, E. Maeder, S. Hempel, M. Butler and V. Mechtcherine, Interphase modification of alkali-resistant glass fibres and carbon fibres for textile reinforced concrete I: fibre properties and durability, *Compos. Sci. Technol.*, 2009, **69**, 531–538, DOI: 10.1016/j.compscitech.2008.12.020.
- 25 M. Malek, M. Jackowski, W. Asica, M. Kadela and M. Wachowski, Mechanical and Material Properties of Mortar Reinforced with Glass Fiber: An Experimental Study, *Materials*, 2021, **14**, 698, DOI: 10.3390/ma14030698.
- 26 M. Sayyar, P. Soroushian, M. M. Sadiq, A. Balachandra and J. Lu, Low-cost glass fiber composites with enhanced alkali resistance tailored towards concrete reinforcement, *Constr. Build. Mater.*, 2013, **44**, 458–463, DOI: 10.1016/j.conbuildmat.2013.03.055.
- 27 Q. Wang, Y. Ding and N. Randl, Investigation on the alkali resistance of basalt fiber and its textile in different alkaline environments, *Constr. Build. Mater.*, 2020, **272**, 121670, DOI: 10.1016/j.conbuildmat.2020.121670.
- 28 S. L. Gao, E. Mäder and R. Plonka, Nanostructured coatings of glass fibers: improvement of alkali resistance and mechanical properties, *Acta Mater.*, 2007, **55**, 1043–1052, DOI: 10.1016/j.actamat.2006.09.020.
- 29 W. Liang, J. Cheng, Y. Hu and L. Hui, Improved properties of GRC composites using commercial E-glass fibers with new coatings, *Mater. Res. Bull.*, 2002, **37**, 641–646, DOI: 10.1016/S0025-5408(02)00700-6.
- 30 B. Taallah and A. Guettala, The mechanical and physical properties of compressed earth block stabilized with lime and filled with untreated and alkali-treated date palm fibers, *Constr. Build. Mater.*, 2016, **104**, 52–62, DOI: 10.1016/j.conbuildmat.2015.12.007.
- 31 R. Guo, S. Jiang, M. Hu, Y. H. Zhan, K. Cheng and G. G. Duan, Adsorption of volatile benzene series compounds by surface-modified glass fibers: kinetics, thermodynamic adsorption efficiencies, and mechanisms, *Environ. Sci. Pollut. Res. Int.*, 2021, **109**, 1–10, DOI: 10.1007/s11356-020-12227-4.
- 32 P. Pouria, R. N. Michelle and B. Dorina, Effect of surface treatment on the post-peak residual strength and toughness of polypropylene/polyethylene-blended fiber-reinforced concrete, *J. Compos. Mater.*, 2011, **45**, 2047–2054, DOI: 10.1177/0021998311399481.
- 33 K. Tosun, B. Felekoğlu and B. Baradan, Multiple cracking response of plasma treated polyethylene fiber reinforced cementitious composites under flexural loading, *Cem. Concr. Compos.*, 2012, **34**, 508–520, DOI: 10.1016/j.cemconcomp.2011.12.001.
- 34 W. Zhang, P. Yang, Y. Cao, P. Yu and X. Zhou, Evaluation of fiber surface modification via air plasma on the interfacial behavior of glass fiber reinforced laminated veneer lumber composites, *Constr. Build. Mater.*, 2020, **233**, 117315, DOI: 10.1016/j.conbuildmat.2019.117315.
- 35 M. I. Siyal, A. A. Khan, C. K. Lee and J. O. Kim, Surface modification of glass fiber membranes by fluorographite coating for desalination of concentrated saline water with humic acid in direct-contact membrane distillation, *Sep. Purif. Technol.*, 2018, **205**, 284–292, DOI: 10.1016/j.seppur.2018.05.045.
- 36 E. Mader, R. Plonka, M. Schiekkel and R. Hempel, Coatings on alkali-resistant glass fibres for the improvement of concrete, *J. Ind. Text.*, 2004, **33**, 191–207, DOI: 10.1177/1528083704039833.
- 37 S. L. Gao, E. Mäder and R. Plonka, Coatings for glass fibers in a cementitious matrix, *Acta Mater.*, 2004, **52**, 4745–4755, DOI: 10.1016/j.actamat.2004.06.028.
- 38 S. A. Mazari, E. Ali, R. Abro, F. S. A. Khan, I. Ahmed, M. Ahmed, S. Nizamuddin, T. H. Siddiqui, N. Hossain, N. M. Mubarak and A. Shah, Nanomaterials: applications, waste-handling, environmental toxicities, and future challenges-A review, *J. Environ. Chem. Eng.*, 2021, **9**, 105028, DOI: 10.1016/j.jece.2021.105028.
- 39 J. Zhang, Study on nano materials of glass fiber surface modification and performance, MS thesis, Tianjin University of Science and Technology, 2015.
- 40 M. Y. Liu, H. G. Zhu, N. A. Siddiqui, C. K. Y. Leung and J. K. Kim, Glass fibers with clay nanocomposite coating: improved barrier resistance in alkaline environment, *Composites, Part A*, 2011, **42**, 2051–2059, DOI: 10.1016/j.compositesa.2011.09.013.
- 41 S. L. Gao, E. Mäder and R. Plonka, Nanocomposite coatings for healing surface defects of glass fibers and improving





- interfacial adhesion, *Compos. Sci. Technol.*, 2008, **68**, 2892–2901, DOI: 10.1016/j.compscitech.2007.10.009.
- 42 B. Wei, S. Song and H. Cao, Strengthening of basalt fibers with nano-SiO<sub>2</sub>-epoxy composite coating, *Mater. Des.*, 2011, **32**, 4180–4186, DOI: 10.1016/j.matdes.2011.04.041.
  - 43 A. Rahaman and K. K. Kar, Carbon nanomaterials grown on E-glass fibers and their application in composite, *Compos. Sci. Technol.*, 2014, **101**, 1–10, DOI: 10.1016/j.compscitech.2014.06.019.
  - 44 F. Mohammadkazemi, K. Doosthoseini, E. Ganjian and M. Azin, Manufacturing of bacterial nano-cellulose reinforced fiber-cement composites, *Constr. Build. Mater.*, 2015, **101**, 958–964, DOI: 10.1016/j.conbuildmat.2015.10.093.
  - 45 W. G. Zhong, M. L. Xin, D. Wang, C. C. Jiang, L. N. Zhang and X. Cheng, Study on in situ modification of poly-dopamine on glass fibers and its effect on shrinkage performance of cement materials, *IOP Conf. Ser.: Mater. Sci. Eng.*, 2020, **770**, 012102, DOI: 10.1088/1757-899X/770/1/012102.
  - 46 E. Diler, B. Rouvellou, S. Rioual, B. Lescop, G. N. Vien and D. Thierr, Characterization of corrosion products of Zn and Zn-Mg-Al coated steel in a marine atmosphere, *Corros. Sci.*, 2014, **87**, 111–117, DOI: 10.1016/j.corsci.2014.06.017.
  - 47 H. P. Zhang, W. Han, J. Tavakoli, Y. P. Zhang, X. Y. Lin, X. Lu, Y. Ma and Y. H. Tang, Understanding interfacial interactions of polydopamine and glass fiber and their enhancement mechanisms in epoxy-based laminates, *Composites, Part A*, 2019, **116**, 62–71, DOI: 10.1016/j.compositesa.2018.10.024.
  - 48 R. A. Zangmeister, T. A. Morris and M. J. Tarlov, Characterization of Polydopamine Thin Films Deposited at Short Times by Autoxidation of Dopamine, *Langmuir*, 2013, **29**, 8619–8628, DOI: 10.1021/la400587j.
  - 49 B. H. Kim, D. H. Lee, J. Y. Kim, D. O. Shin, H. Y. Jeong, S. Hong, J. M. Yun, C. M. Koo, H. Lee and S. O. Kim, Mussel-Inspired Block Copolymer Lithography for Low Surface Energy Materials of Teflon, Graphene, and Gold, *Adv. Mater.*, 2011, **23**, 5618–5622, DOI: 10.1002/adma.201103650.
  - 50 J. S. Stevens, S. J. Byard, C. C. Seaton, G. Sadiq, R. J. Davey and S. L. M. Schroeder, Proton transfer and hydrogen bonding in the organic solid state: a combined XRD/XPS/ssNMR study of 17 organic acid-base complexes, *Phys. Chem. Chem. Phys.*, 2014, **16**, 1150–1160, DOI: 10.1039/C3CP53907E.
  - 51 Z. X. Han, Y. Q. Ni, W. F. Zhang, Y. F. Wang, Z. Xie, S. Y. Zhou and S. F. Yu, Highly efficient and ultra-narrow bandwidth orange emissive carbon dots for microcavity lasers, *Nanoscale*, 2019, **11**, 11577–11583, DOI: 10.1039/C9NR03448J.
  - 52 H. W. Kim, B. D. McCloskey, T. H. Choi, C. Lee, M. J. Kim, B. D. Freeman and H. B. Park, Oxygen concentration control of dopamine-induced high uniformity surface coating chemistry, *ACS Appl. Mater. Interfaces*, 2013, **5**, 233–238, DOI: 10.1021/am302439g.
  - 53 M. Rezaia, H. Moradnezah, M. Panahandeh, M. J. R. Kami and B. V. Hosseini, Effects of Diethanolamine (DEA) and Glass Fibre Reinforced polymer (GFRP) on setting time and mechanical properties of shotcrete, *J. Build. Eng.*, 2020, **31**, 101343, DOI: 10.1016/j.jobbe.2020.101343.
  - 54 M. Malek, M. Jackowski, W. Asica, M. Kadela and M. Wachowski, Mechanical and Material Properties of Mortar Reinforced with Glass Fiber: An Experimental Study, *Materials*, 2021, **14**, 698, DOI: 10.3390/ma14030698.
  - 55 X. Y. Zhou, Y. S. Zeng, P. Chen, Z. Z. Jiao and W. Z. Zheng, Mechanical properties of basalt and polypropylene fibre-reinforced alkali-activated slag concrete, *Constr. Build. Mater.*, 2021, **269**, 121284, DOI: 10.1016/j.conbuildmat.2020.121284.
  - 56 Z. Yuan and Y. Jia, Mechanical properties and microstructure of glass fiber and polypropylene fiber reinforced concrete: an experimental study, *Constr. Build. Mater.*, 2021, **266**, 121048, DOI: 10.1016/j.conbuildmat.2020.121048.
  - 57 M. H. Zhang, M. Q. Jiang and J. K. Chen, Variation of flexural strength of cement mortar attacked by sulfate ions, *Eng. Fract. Mech.*, 2008, **75**, 4948–4957, DOI: 10.1016/j.engfracmech.2008.06.023.
  - 58 R. Poorhosein and M. Nematzadeh, Mechanical behavior of hybrid steel-PVA fibers reinforced reactive powder concrete, *Comput. Concr.*, 2018, **21**, 167–179, DOI: 10.12989/cac.2018.21.2.167.
  - 59 K. L. Scrivener, J. L. Cabiron and R. Letourneux, High-performance concretes from calcium aluminate cements, *Cem. Concr. Res.*, 1999, **29**, 1215–1223, DOI: 10.1016/S0008-8846(99)00103-9.
  - 60 W. Abbass, M. I. Khan and S. Mourad, Evaluation of mechanical properties of steel fiber reinforced concrete with different strengths of concrete, *Constr. Build. Mater.*, 2018, **168**, 556–569, DOI: 10.1016/j.conbuildmat.2018.02.164.

